PNAS RESEARCH ARTICLE | IMMUNOLOGY AND INFLAMMATION

CD47 and thrombospondin-1 contribute to immune evasion by *Porphyromonas gingivalis*

Sarah Angabo[a], Karthikeyan Pandi[a], Keren David[a], Orit Steinmetz[a], Hasnaa Makkawi[a], Maria Farhat[a], Luba Eli-Berchoer[a], Nadeem Darawshi[a], Hiromichi Kawasaki[a,b], and Gabriel Nussbaum[a,1]

Affiliations are included on p. 10.

Edited by Thomas E. Van Dyke, Harvard University, Cambridge, MA; received March 17, 2024; accepted September 25, 2024 by Editorial Board Member Carl F. Nathan

Porphyromonas gingivalis **is a gram-negative anaerobic bacterium linked to periodontal disease. Remarkably,** ***P. gingivalis*** **thrives in an inflamed environment rich in activated neutrophils. Toll-like receptor 2 (TLR2) recognition is required for** ***P. gingivalis*** **to evade innate immune killing; however, the mechanisms through which** ***P. gingivalis*** **uncouples host inflammation from bactericidal activity are only partially known. Since integrin activation and alternative signaling are implicated in** ***P. gingivalis*** **TLR2-mediated immune escape, we explored the role of CD47, a widely expressed integrin-associated protein known to suppress phagocytosis and implicated as an interacting partner with other innate immune receptors. We found that CD47 associates with TLR2, and blocking CD47 leads to decreased intracellular** ***P. gingivalis*** **survival in macrophages in a manner dependent on the bacterial major fimbria. In vivo, CD47 knock-out mice cleared** ***P. gingivalis*** **more efficiently than wild-type mice. Next, we found increased expression and secretion of the CD47 ligand thrombospondin-1 (TSP-1) following** ***P. gingivalis*** **infection. Secreted TSP-1 broadly protected** ***P. gingivalis*** **and other periodontitis-associated bacterial species from neutrophil bactericidal activity. Therefore, CD47-TLR2 cosignaling in response to** ***P. gingivalis*** **induces TSP-1 that in turn suppresses neutrophil activity, an effect that can explain how species such as** ***P. gingivalis*** **survive in an inflamed environment and cause dysbiosis.**

CD47 | thrombospondin-1 | *Porphyromonas gingivalis* | immune evasion

Some bacterial species thrive in inflamed mucosal tissue, and to do so, they rely on mechanisms that uncouple inflammatory signaling in innate immune cells from responses that promote bacterial killing (1). *Porphyromonas gingivalis*, an anaerobic gram-negative bacterium linked to periodontal disease, is a prime example. *P. gingivalis* load increases as the oral soft tissue surrounding the teeth becomes more inflamed (2). To escape innate immune clearance, *P. gingivalis* relies on a pathway that requires phosphoinositide-3-kinase (PI3K) activation downstream of the pattern recognition receptor Toll-like receptor (TLR) 2 (3–5). Remarkably, the absence or inhibition of TLR2 restores efficient macrophage and neutrophil antibacterial activity (6, 7). Since TLR2 canonical signaling proceeds through the intracellular adapter protein MyD88, how *P. gingivalis* circumvents this signaling pathway and favors PI3K-AKT signaling is key to understanding its evasion strategy. What is clear is that TLR2 does not act alone; multiple additional membrane proteins participate together with TLR2 in the response to *P. gingivalis*, including the C5a and C3 complement receptors (8, 9), CXC chemokine receptor 4 (10, 11), and integrins (12, 13). In the current work, we hypothesized that the integrin-associated protein (IAP) CD47 participates in the immune escape pathway of *P. gingivalis*. The key findings supporting this hypothesis are as follows: 1) CD47 plays a known role in regulating phagocytosis and has been proposed as a checkpoint in the host response to pathogens (14, 15), 2) TLR2/CD47 costimulation regulates neutrophil transmigration (16), 3) macrophages from inflamed periodontal tissue overexpress CD47 (17), and 4) CD47 interacts with integrin family members such as αvβ3 that are implicated in the response to *P. gingivalis* and other TLR2 ligands (12, 18–20).

In addition to its interactions with integrins, CD47 serves as a receptor for thrombospondins and for the inhibitory cell-surface receptor signal regulatory protein alpha (SIRPα) (21, 22). Both of these interactions have been implicated in modulating the host response to infection (23, 24). In addition to its known role in cancer cell immune evasion, CD47 interaction with SIRPα suppresses phagocytosis and modulates innate and adaptive immune responses (25, 26). Thrombospondin-1 (TSP-1) is a secreted

Significance

Microbe-driven chronic inflammation in the oral cavity leads to periodontitis, a risk for systemic diseases. *Porphyromonas gingivalis* is a bacterial species that thrives alongside activated immune cells in periodontitis and has been linked to cardiovascular disease, Alzheimer's, and cancer. *P. gingivalis* is detected by Toll-like receptor 2 (TLR2); however, downstream signaling uncouples inflammation from bactericidal activity. Here, we identified CD47, an integrin-associated protein, as an interacting partner of TLR2. CD47 is co-opted by *P. gingivalis* for survival since bacterial clearance is enhanced in its absence. We found that *P. gingivalis* induces the CD47 ligand thrombospondin-1 (TSP-1) that broadly suppresses neutrophil activity against periodontitis-associated bacterial species. Blocking TLR2–CD47 cosignaling or TSP-1 represents a uniqueapproach to control *P. gingivalis*–related pathologies.

Author contributions: S.A., K.D., and G.N. designed research; S.A., K.P., K.D., O.S., H.M., M.F., L.E.-B., N.D., H.K., and G.N. performed research; S.A., K.P., K.D., O.S., H.M., and G.N. analyzed data; and S.A. and G.N. wrote the paper.

The authors declare no competing interest.

This article is a PNAS Direct Submission. T.E.V.D. is a guest editor invited by the Editorial Board.

[1]To whom correspondence may be addressed. Email: gabrieln@ekmd.huji.ac.il.

This article contains supporting information online at https://www.pnas.org/lookup/suppl/doi:10.1073/pnas.2405534121/-/DCSupplemental.

Published November 13, 2024.

factor that interacts with CD47 as well as additional innate immune receptors and can promote or regulate inflammation in a context-dependent manner (27, 28). Several studies have found that *P. gingivalis* induces TSP-1 production and blocking TSP-1 in models of periodontitis reduces disease outcomes (29, 30). We therefore explored the role of CD47 and its ligands in the innate response to *P. gingivalis*.

Periodontal disease affects over a third of the adult population (31). In periodontal disease, tooth brushing induces transient bacteremia with *P. gingivalis* and other periodontitis-associated bacteria (32), enabling bacteria to translocate to distant sites. Extraoral *P. gingivalis* contributes to a range of diseases, including cancer and Alzheimer's disease (33–35). Our study highlights the contribution of CD47 and TSP-1 to the evasion mechanism that enables *P. gingivalis* to thrive in an inflammatory milieu, and suggests that blocking this pathway represents a unique strategy to improve health outcomes.

Results

CD47 Contributes to *P. gingivalis* Evasion from Bacterial Killing. To explore the role of CD47 in the evasion strategy of *P. gingivalis*, we blocked CD47 using a neutralizing antibody prior to infection of human or mouse macrophages. To focus on intracellular bactericidal activity, after a 1 h infection period extracellular bacteria were eliminated by treatment with metronidazole and gentamicin (1 h) (36). Surviving intracellular bacteria were enumerated after a further 1 h incubation. Despite a small reduction in macrophage phagocytosis (*SI Appendix*, Fig. S1*A*), macrophage clearance of internalized bacteria was significantly improved by blocking CD47 (Fig. 1 *A* and *B*). Since *P. gingivalis* major fimbriae interact with integrin family members (β1 and β3 integrins) that associate with, and activate CD47, (12) we tested CD47 involvement in macrophage bactericidal activity in the absence of bacterial fimbriae. The major *P. gingivalis* fimbria

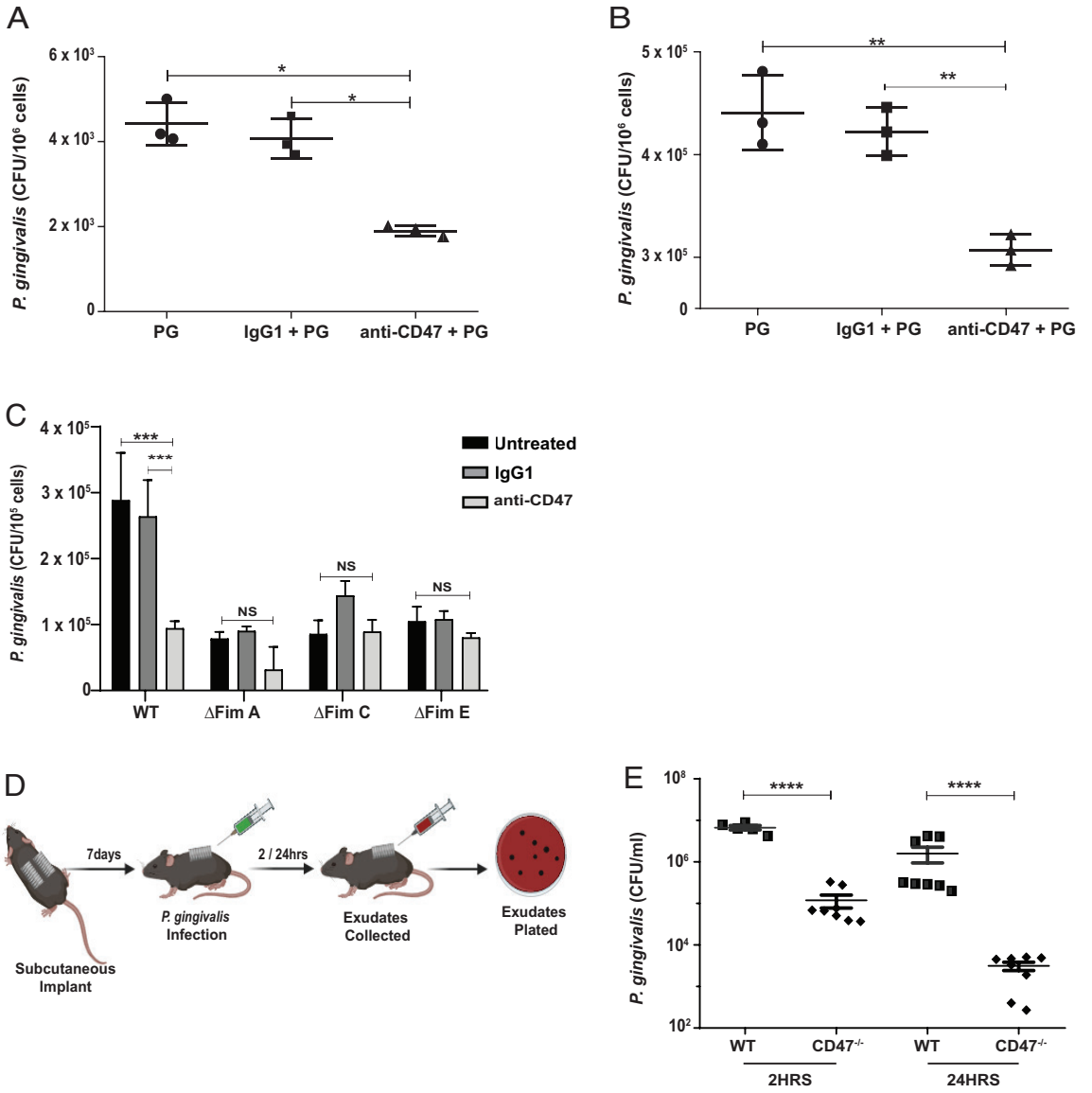

Fig. 1. CD47 promotes *P. gingivalis* survival in vitro and in vivo. THP-1 (*A*) and Raw 264.7 (*B*) macrophages were treated with blocking antibodies to CD47 or IgG control (10 μg/mL), followed by *P. gingivalis* (PG) infection (MOI 10). The intracellular bacterial survival assay was performed, and bacterial colonies were determined. Data of one representative experiment of three are shown. (*C*) THP-1 macrophages were pretreated with blocking antibodies to CD47 or IgG control. Cells were infected with ATCC strain 33277 (WT) or fimbria-mutant PG for 1 h. Intracellular bacterial survival was determined. (*D*) Graphical representation of in vivo experimental model. (*E*) Viable PG counts were determined following infection of WT and CD47$^{-/-}$ mice. Each dot represents an individual mouse. One representative experiment of two is shown. (*A* and *B*) One-way ANOVA, (*C*) two-way ANOVA, and (*E*) two-tailed *t* test were performed to determine statistical significance (ns: nonsignificant, *$P < 0.05$; **$P < 0.01$; ***$P < 0.001$; ****$P < 0.0001$).

is composed of a shaft encoded by the *fima* gene, and accessory proteins encoded by *fimc-e* genes. *P. gingivalis* deletion mutants ΔFimA, ΔFimC, and ΔFimE are cleared more efficiently by macrophages compared to wild-type (WT) bacteria [as previously shown (37)], and in this case blocking CD47 has no effect on macrophage bactericidal activity (Fig. 1*C*), consistent with a role for the major fimbriae in activation of CD47. We next hypothesized that CD47 plays a global role in *P. gingivalis* immune evasion in vivo. Since neutrophils constitute the majority of phagocytes that *P. gingivalis* encounters in its natural niche, the periodontal pocket, we determined the role of CD47 in *P. gingivalis* evasion of neutrophil-mediated clearance in WT vs. CD47 deficient mice. To this end, we used an infection model in which bacteria are inoculated into the lumen of titanium-coil chambers implanted subcutaneously 10 days prior to bacterial challenge (38, 39). In this model the majority of chamber cells are neutrophils, and monocyte/macrophages constitute a minority population that actively down-regulate neutrophil-mediated killing of *P. gingivalis* (39). Bacterial clearance is determined by measuring *P. gingivalis* colony-forming units (CFU) in the chamber exudate postinfection

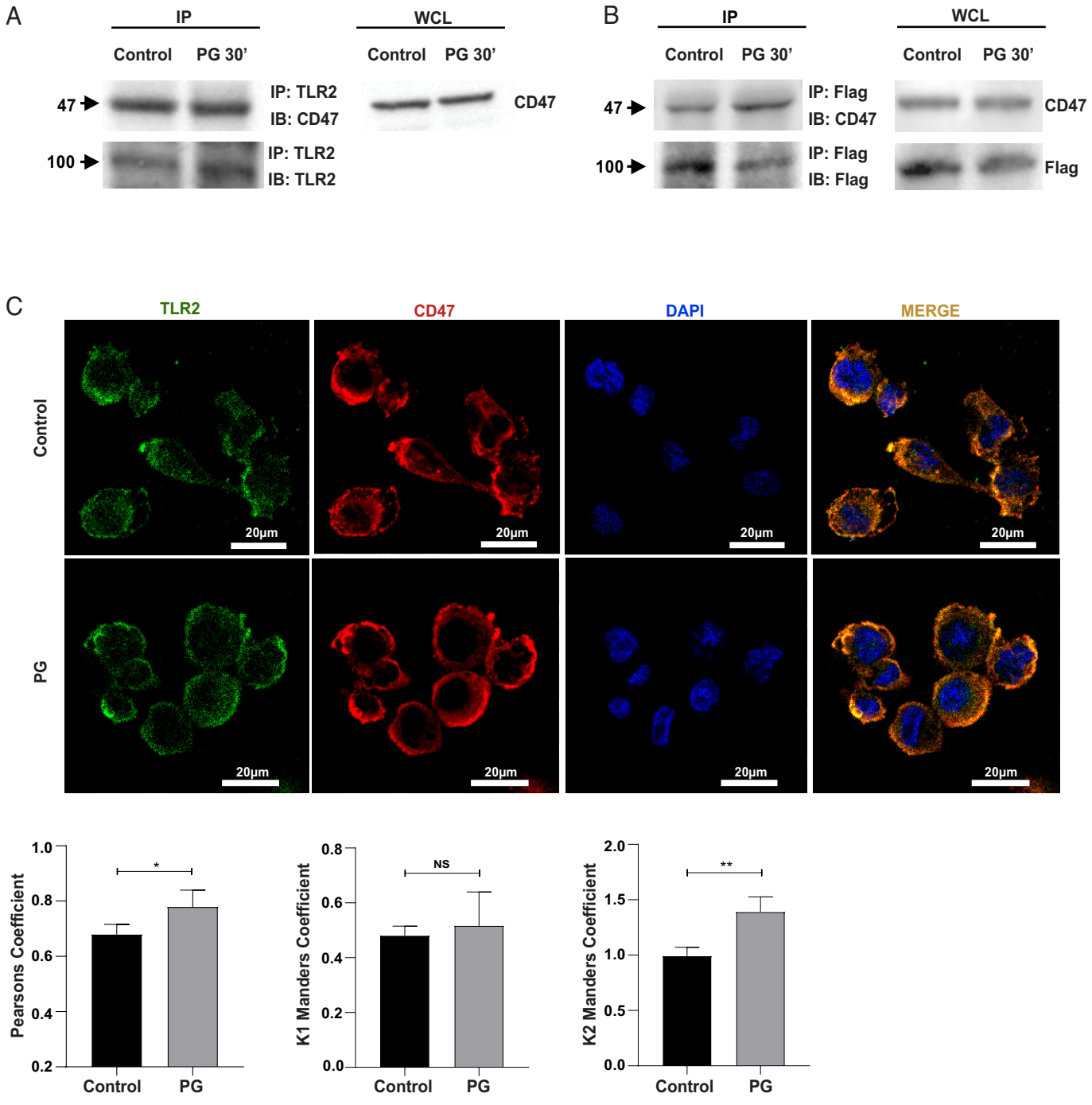

Fig. 2. CD47 associates with TLR2. (*A*) THP-1 macrophages and (*B*) TLR2-Flag overexpressing THP-1 macrophages were infected with *P. gingivalis* (PG, MOI 10) for 30 min. TLR2 was IP with anti-TLR2 (*A*) or anti-Flag (*B*), and eluates were analyzed for CD47 (*A* and *B*), TLR2 (*A*), or TLR2-Flag (*B*) by immunoblot (IB). CD47 and TLR2-Flag protein levels in whole cell lysates (WCL) were also determined (no native TLR2 was detected in the THP-1 WCL). (*C*) THP-1 macrophages were infected with PG for 30 min, fixed, and stained for TLR2 (green) and CD47 (red). Nuclei were stained with DAPI (blue) and merged images were used to evaluate colocalization of TLR2 and CD47. Images were obtained using a Nikon confocal microscope at 40× magnification and colocalization coefficients were determined using ImageJ analysis software. Data are representative of two individual experiments. Two-tailed *t* test analysis was performed (ns: nonsignificant; *$P \leq 0.05$; **$P \leq 0.01$).

(Fig. 1*D*). At 2 and 24 h after inoculation with *P. gingivalis*, bacterial clearance was significantly improved in mice deficient in CD47 (Fig. 1*E*). Therefore, in addition to protecting *P. gingivalis* in macrophages, CD47 is important for bacterial escape from killing by recruited neutrophils in vivo.

CD47 Associates with TLR2 and Influences Signaling in Response to Infection. Given the functional role of TLR2 and CD47 in the response to *P. gingivalis*, we next asked whether the two proteins associate. We found that CD47 immunoprecipitated (IP) with TLR2 in differentiated human THP-1 macrophages at baseline, and the association was not significantly changed in response to *P. gingivalis* infection (Fig. 2*A*). We confirmed the coimmunoprecipitation of CD47 with TLR2 in THP-1 macrophages overexpressing Flag-tagged TLR2 (40); in these cells as well, infection did not significantly increase the association (Fig. 2*B*). Immunofluorescence also demonstrates the colocalization of TLR2 and CD47 in THP-1 macrophages, with infection enhancing the colocalization although not across all measures (Fig. 2*C*). Since *P. gingivalis* infection induces the transcription of TLR2 (41) and other proteins involved in TLR2 signaling (5), we next examined whether CD47 expression is similarly up-regulated by infection. Although infection up-regulated CD47 mRNA in human (THP-1 cells, Fig. 3*A*) and murine (RAW 264.7 cells, Fig. 3*C*) macrophages, surface CD47 expression was unaffected in the human cells and only slightly increased in the murine cells (Fig. 3 *B* and *D*). Similarly, peripheral blood–derived macrophage CD47 baseline expression was strong and was not enhanced by infection despite upregulation of the mRNA levels (Fig. 3 *E* and *F*). In comparison, CD47 transcription by neutrophils was enhanced by *P. gingivalis* infection, and surface protein expression significantly increased in a portion of the cells (Fig. 3 *G* and *H*).

To determine how CD47 influences TLR2 signaling in response to *P. gingivalis* infection, we examined TNF production by macrophages. Blocking TLR2 strongly reduced cytokine production in response to *P. gingivalis* as previously found (3). However, blocking CD47 on human and murine macrophages had no effect (Fig. 4 *A* and *B*). TNF production reflects signaling events that enable nuclear translocation of the NFκB p65 transcription factor. To confirm, we tracked p65 nuclear translocation in macrophages challenged with *P. gingivalis* (Fig. 4*C*). Blocking TLR2, but not CD47, inhibited p65 nuclear translocation. *P. gingivalis* survival in macrophages depends on TLR2 activation of the PI3K/Akt pathway (3). Consistent with the role of CD47 in *P. gingivalis* evasion from macrophage killing (Fig. 1 *A* and *B*), blocking CD47 strongly inhibited AKT phosphorylation induced by *P. gingivalis*

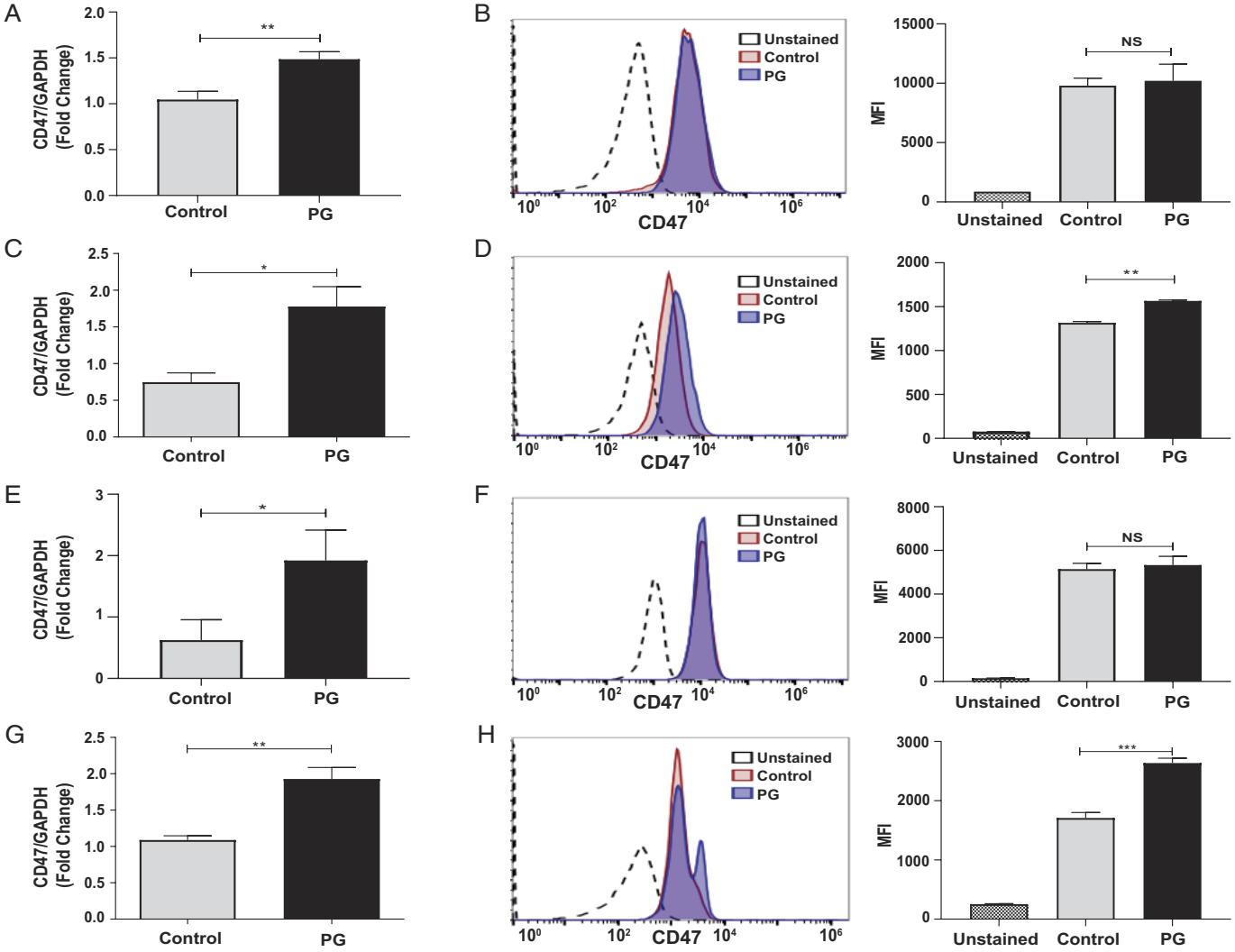

Fig. 3. *P. gingivalis* influences CD47 expression. CD47 expression at baseline and in response to *P. gingivalis* (MOI 10) was measured by qRT-PCR after 4 h of challenge and flow cytometry after 24 h challenge. (*A* and *B*) THP-1, (*C* and *D*) Raw 264.7 macrophages, (*E* and *F*) human PBMC-derived macrophages, and (*G* and *H*) human peripheral blood neutrophils. Data are representative of two to four individual experiments. A two-tailed *t* test was used to analyze differences between groups (ns: nonsignificant; **P* ≤ 0.05; ***P* ≤ 0.01; ****P* < 0.001).

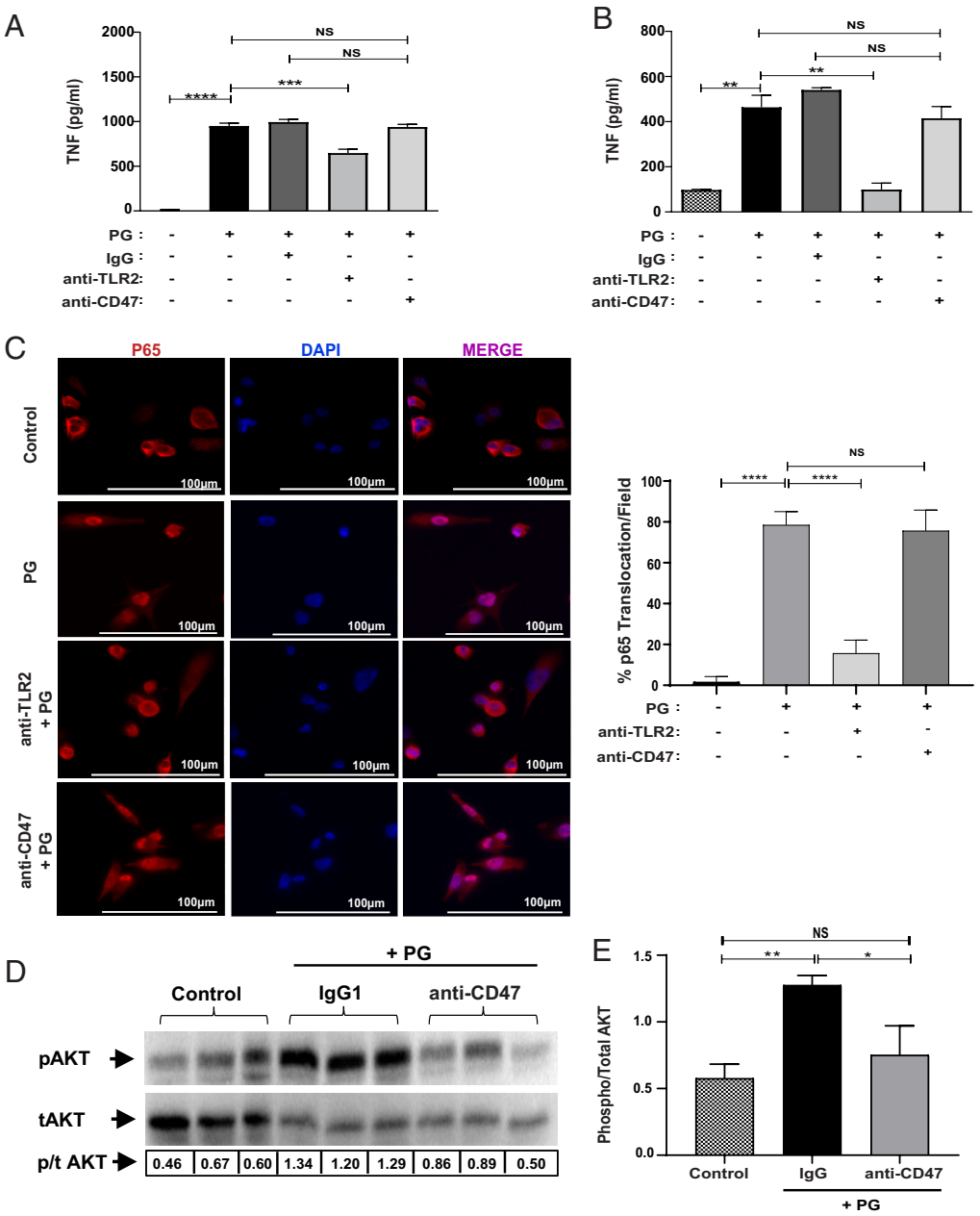

Fig. 4. CD47 mediates *P. gingivalis*–induced AKT phosphorylation but not cytokine production and NFκB translocation. THP-1 (*A*) and Raw 264.7 (*B*) macrophages were pretreated with blocking antibodies to CD47 or TLR2, or IgG control. Cells were infected with *P. gingivalis* (PG, MOI 10) overnight, and cytokine levels were analyzed by the ELISA. (*C*) THP-1 macrophages were infected with PG (MOI 10) for 2 h, fixed, and stained with antibody to p65. Percentage nuclear translocation was determined per field. (*D*) THP-1 macrophages were infected with PG (MOI 20) for 10 min, and phosphorylated and total AKT levels were determined. (*E*) Densitometry graph of phospho/total ratios of *D*. Data are representative of three independent experiments. Statistical significance was determined using one-way ANOVA (ns: nonsignificant, **P* < 0.05; ***P* < 0.01; ****P* < 0.001; *****P* < 0.0001).

infection (Fig. 4*D*). Therefore, *P. gingivalis* activates a TLR2–CD47 complex and the involvement of CD47 expands the signaling events that occur following infection.

***P. gingivalis* Induces TSP-1 Production.** We next asked whether ligands of CD47 may further drive *P. gingivalis* immune escape by enhancing the PI3K/AKT signaling pathway. We tested the effect of infection with *P. gingivalis* on the expression of TSP-1 and SIRP-α, two known CD47 ligands (42). Although expression of SIRP-α was unaffected by *P. gingivalis* infection (Fig. 5 *A* and *B*), TSP-1 mRNA expression was significantly up-regulated in human and murine macrophages (Fig. 5 *C*–*E*), and to a lesser extent in human neutrophils (Fig. 5*F*). TSP-1 protein production was also detectable 6 h and 24 h postinfection with *P. gingivalis* (Fig. 5*G*), and in response to a range of multiplicity of infections (MOIs) (Fig. 5*F*). In contrast to the lack of effect on cytokine production (Fig. 4 *A* and *B*), blocking either CD47 or TLR2 significantly decreased TSP-1 expression (Fig. 5*I*). Similarly, deletion of FimA, or the fimbrial accessory proteins FimC/FimE, abrogates TSP-1 induction, consistent with the role of *P. gingivalis* fimbria in CD47 activation (*SI Appendix*, Fig. S2 *A* and *B*). Inhibition of both NFκB and PI3K signaling pathways blocked TSP-1 induction (Fig. 5 *J* and *K*), suggesting that NFκB is necessary but not sufficient to stimulate TSP-1 expression. Taken together, the involvement of CD47 in the TLR2-driven response to *P. gingivalis* enhances PI3K/AKT signaling, leading to bacterial survival in macrophages, and also to the induction of TSP-1 production. As a secreted factor, TSP-1 can potentially contribute to bacterial immune escape by

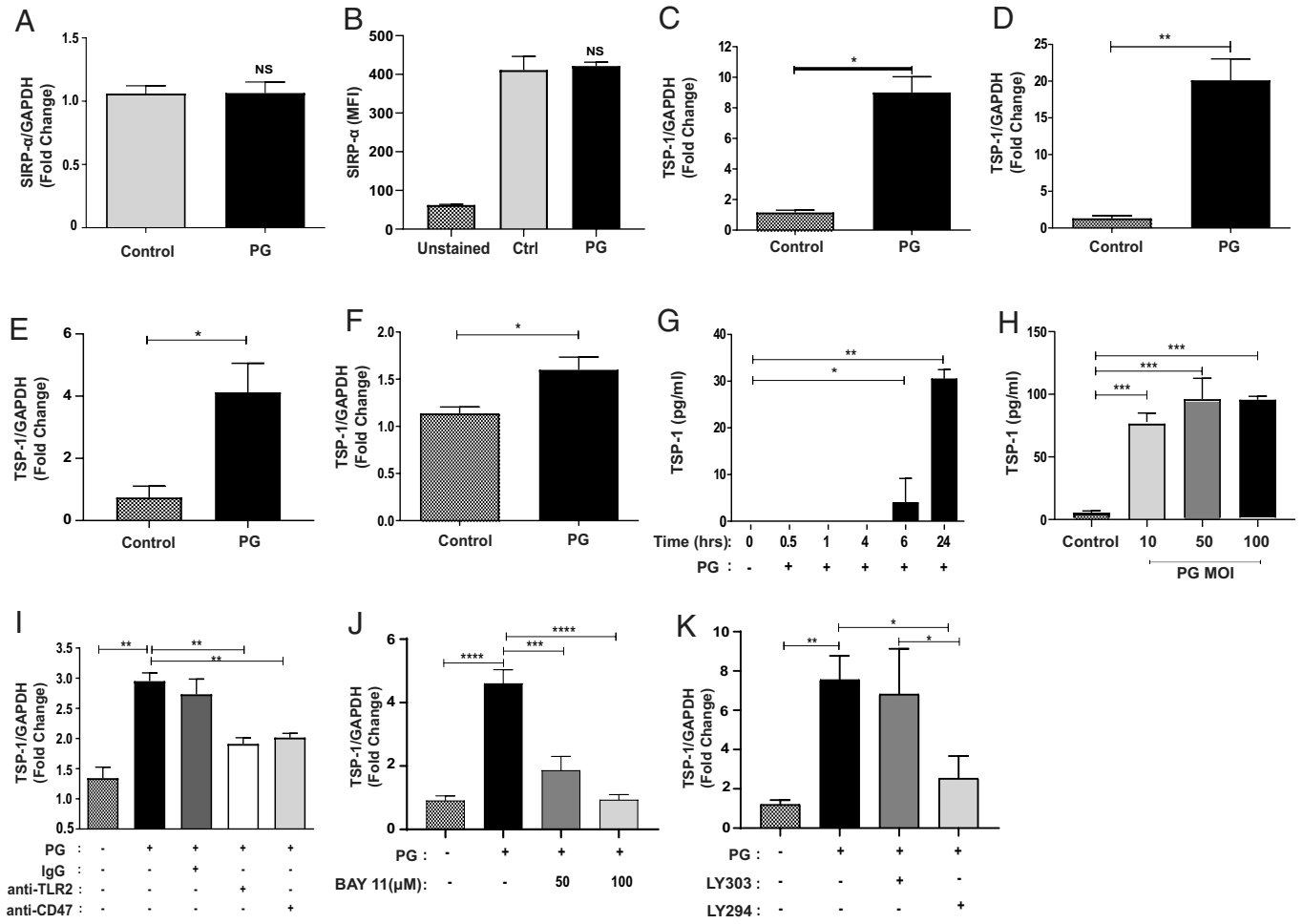

Fig. 5. *P. gingivalis* induces TSP-1 production in a CD47- and TLR2-dependent manner. SIRP-α mRNA (*A*) and protein levels (*B*) were determined after *P. gingivalis* (PG) infection for 4 h and 24 h, respectively. TSP-1 mRNA expression was measured in response to PG infection (4 h, MOI 10) in (*C*) THP-1 macrophages, (*D*) Raw 264.7 macrophages, (*E*) PBMC-derived macrophages, and (*F*) peripheral blood neutrophils. (*G*) TSP-1 protein expression was determined by the ELISA after PG infection at different time points and, (*H*) 24 h after infection with different PG MOI (10, 50, and 100) in THP-1 macrophages. (*I*) THP-1 macrophages were pretreated with blocking antibodies for CD47 or TLR2, or IgG control. TSP-1 mRNA levels were then determined by qRT-PCR after 4 h of PG infection. (*J* and *K*) THP-1 macrophages were pretreated with the NFκB inhibitor (Bay11) (*J*) or PI3K inhibitor (LY294; 100 μM) or its control inactive analogue (LY303; 100 μM) for 1 h. Cells were then infected with PG MOI 10 for 4 h. TSP-1 mRNA levels were determined by qRT-PCR. Data are representative of two-three individual experiments. Two-tailed *t* test analysis (*A*–*D*, *G*, and *H*) and one-way ANOVA (*E*, *F*, and *I*) were performed (ns: nonsignificant; $^*P \le 0.05$; $^{**}P \le 0.01$; $^{***}P < 0.001$; $^{****}P < 0.0001$).

engaging CD47 broadly on cells that have not yet encountered bacteria (Fig. 1*D*).

TSP-1 Down-Regulates Neutrophil Bactericidal Activity. To evaluate this possibility, we pretreated human neutrophils with TSP-1 prior to challenge with *P. gingivalis*. TSP-1 treatment reduced neutrophil phagocytosis of *P. gingivalis* (Fig. 6*A*). To understand the effect of TSP-1 on intracellular bactericidal activity, we removed extracellular bacteria by washing and treatment with gentamicin and metronidazole for 1 h. Neutrophils were rested for an hour and then lysed, and lysates were plated on blood agar to enumerate intracellular surviving CFU. Despite a reduced intracellular load due to decreased phagocytosis (Fig. 6*A*), significantly more surviving bacteria were recovered from TSP-1-treated neutrophils (Fig. 6*B*). To understand how TSP-1 protects phagocytosed *P. gingivalis*, induction of reactive oxygen species (ROS) in response to infection was evaluated. As expected, infection strongly induced neutrophil ROS production; however, pretreatment with TSP-1 reduced the ROS level to background (Fig. 6*C*). To confirm that the downregulation of neutrophil ROS by TSP-1 results from activation of neutrophil CD47, we blocked the interaction of TSP-1 with CD47 using a cyclic peptide inhibitor [TAX2 peptide (43), Fig. 6*D*]. Preincubation with TAX2 completely restored neutrophil bactericidal activity (Fig. 6*E*), and ROS production (Fig. 6*F*), in cells treated with TSP-1 prior to infection.

TSP-1 Protects Periodontitis-Associated Bacteria from Neutrophil-Mediated Killing. Periodontitis lesions are infiltrated with neutrophils that do not efficiently clear bacteria. TSP-1 has been shown to be elevated in the inflamed tissue of human periodontitis patients (44), and we therefore evaluated its ability to play a general role in bacterial escape from neutrophil killing. First, we found that additional periodontitis-associated bacterial species, *Tannerella forsythia* and *Fusobacterium nucleatum*, induced TSP-1 gene expression, and protein secretion, in human macrophages (Fig. 7 *A* and *B*). CD47 also plays a role in the immune evasion of these pathogens that are known to activate TLR2 (45–47) (*SI Appendix*, Fig. S3 *A* and *B*). We next evaluated the role of TSP-1 in neutrophil antibacterial activity against these pathogens. Unlike for *P. gingivalis*, phagocytosis of *T. forsythia* and *F. nucleatum* was unaffected by TSP-1 treatment (*SI Appendix*, Fig. S4 *A* and *B*). Notably, human neutrophils efficiently cleared *T. forsythia*; however, pretreatment with TSP-1 reversed this effect, enabling *T. forsythia* intracellular survival (Fig. 7*C*). Neutrophil TSP-1 treatment also promoted intracellular survival of *F. nucleatum* (Fig. 7*D*). Thus, TSP-1 is a soluble factor that has

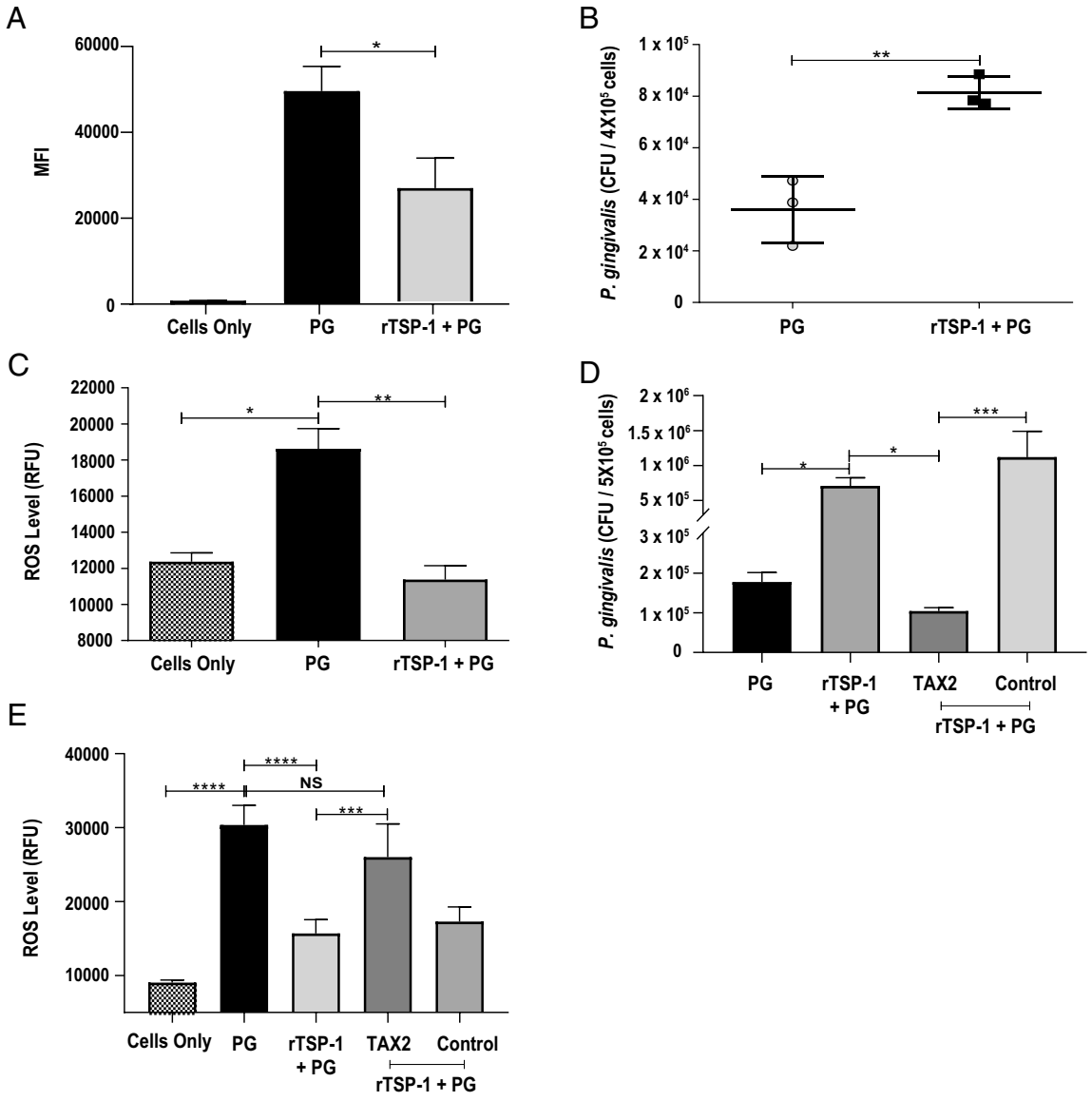

Fig. 6. TSP-1 down-regulates neutrophil bactericidal activity. (*A*) Peripheral blood neutrophils were pretreated with recombinant (r) TSP-1 (100 ng/mL) for 30 min and cells were then infected with FITC-labeled *P. gingivalis* (PG) for 30 min. Phagocytosis was determined by flow cytometry. (*B* and *C*) Neutrophils were treated with rTSP-1 (100 ng/mL) for 30 min and then infected with *P. gingivalis* for 1 h. Viable intracellular PG were determined after antibiotic treatment to remove extracellular bacteria (*B*). ROS levels were determined by Dihydrorhodamine 123 (DHR-123) (*C*). (*D* and *E*) Neutrophils were pretreated with TAX2 peptide or scrambled peptide control (100 μM) for 1 h prior to rTSP-1 (100 ng/mL) for 30 min and PG infection (MOI 10) for 1 h. Intracellular survival (*D*) and ROS levels (*E*) were determined. Data are representative of three individual experiments. Two-tailed *t* test (*A* and *B*) and one-way ANOVA (*C*–*E*) were performed to determine statistical significance (ns: nonsignificant, **P* < 0.05; ***P* < 0.01; ****P* < 0.001; *****P* < 0.0001).

broad protective effects for bacteria associated with periodontal disease (schematically represented in Fig. 8).

Discussion

In the innate immune system, a limited set of TLRs recognize and respond to a diverse array of microbial and damage-associated ligands. Accessory proteins and cofactors that bind to TLR homo- or heterodimers help explain the variation in ligands that TLRs detect (48); however, surface proteins that complex with TLRs also diversify the signaling pathways downstream of TLR activation and thereby open opportunities for pathogens to manipulate host responses. For *P. gingivalis*, an asaccharolytic organism that thrives in the presence of tissue breakdown products provided by inflammation, surface receptors such as the complement C5a receptor (C5aR) were shown to protect bacteria while cooperating with TLR2 to promote inflammation (9). In a similar manner, we now found that CD47-TLR2 cosignaling facilitates *P. gingivalis* survival. *P. gingivalis* fimbriae are critical for this activation, consistent with the known interaction of fimbriae with integrin family members (β1 and β3 integrins) that associate with, and activate, CD47 (10, 12, 20, 49). Since TLR2 is integral to the macrophage response to *P. gingivalis* (3, 7, 11, 50), blocking TLR2 shuts down cytokine and TSP-1 induction. However, blocking antibodies to CD47 do not interfere with the cytokine response to infection, and the lack of steric hindrance suggests that TLR2 and CD47 interact indirectly via integrins as part of a protein complex (5, 40). CD47 functions as part of a supramolecular complex that includes heterotrimeric G proteins known to signal through PI3K-AKT (51). Notably, blocking CD47 reduces AKT phosphorylation in response to *P. gingivalis* without inhibiting p65 nuclear translocation. Therefore, *P. gingivalis* can engage PI3K-AKT signaling via the CD47-TLR2 association, representing a protein–protein complex that expands the possible outcome

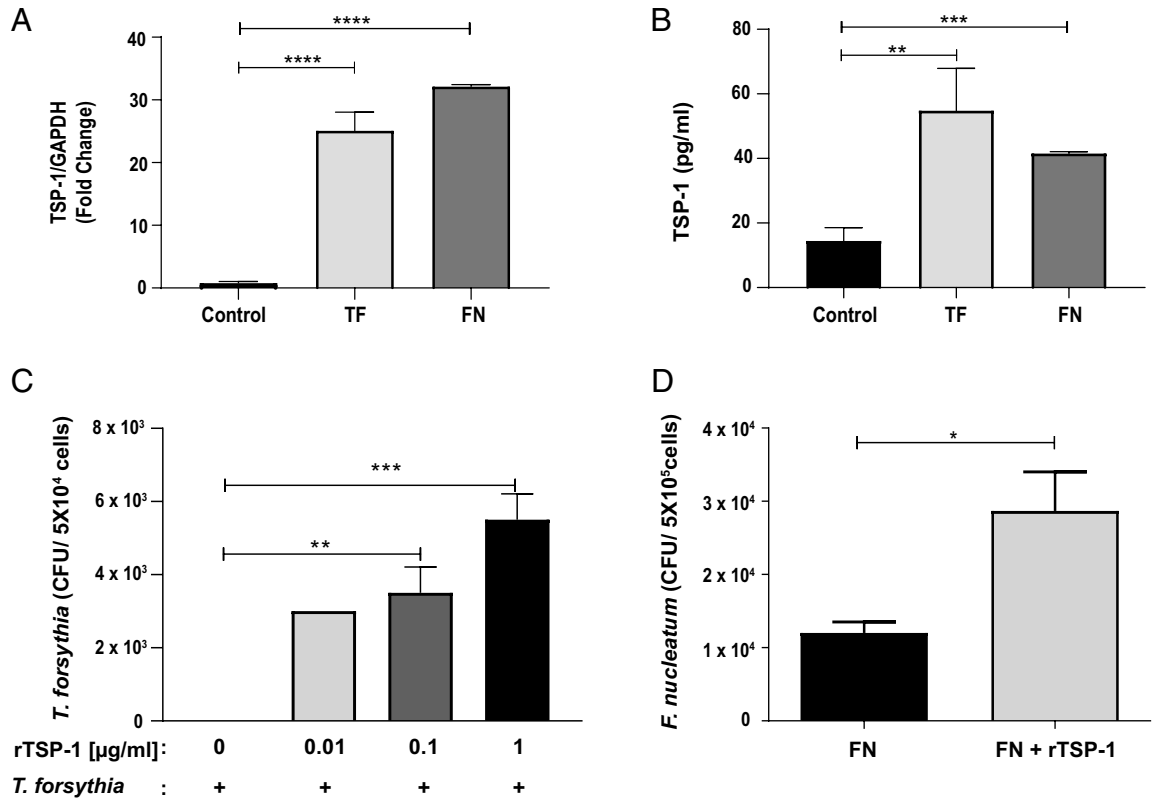

Fig. 7. TSP-1 protects periodontal pathogens from neutrophil-mediated killing. (*A*) THP-1 macrophages were infected with *F. nucleatum* (FN, MOI 10) or *T. forsythia* (TF, MOI 10) for 4 h, and TSP-1 mRNA expression was determined. (*B*) TSP-1 protein after overnight infection of THP-1 macrophages with FN (MOI 10) or TF (MOI 10). (*C*) Peripheral blood neutrophils were pretreated with rTSP-1 at varying concentrations for 30 min. Cells were then infected with TF (MOI 10) for 1 h. Intracellular bacteria survival was determined. (*D*) Neutrophils were pretreated with rTSP-1 (100 ng/mL) for 30 min. Cells were then infected with FN (MOI 2) for 1 h and intracellular survival was determined. Data are representative of three individual experiments. Two-tailed *t* test (*A*, *B*, and *D*) and one-way ANOVA (*C*) were used to determine statistical significance (ns: nonsignificant, *$P < 0.05$; **$P < 0.01$; ***$P < 0.001$; ****$P < 0.0001$).

of TLR2-mediated responses (5, 40). Blocking CD47 improved macrophage killing of additional bacterial species that interact with TLR2, suggesting that the CD47-TLR2 association may contribute broadly to bacterial immune evasion. Since macrophage CD47-TLR2 association is constitutive (Fig. 2 *A* and *B*), activation of CD47 is possible without priming or generation of additional ligands, distinguishing it from the activation of C5aR that requires proteolytic cleavage of C5 (9). *P. gingivalis* infection also induces secretion of the matrix glycoprotein TSP-1 that can augment CD47 signaling (49) and bacterial immune escape. In addition to immune effects, TSP-1 was shown to induce periodontal ligament fibroblasts to produce matrix metalloproteinases (29), further promoting tissue destruction and facilitating bacterial overgrowth.

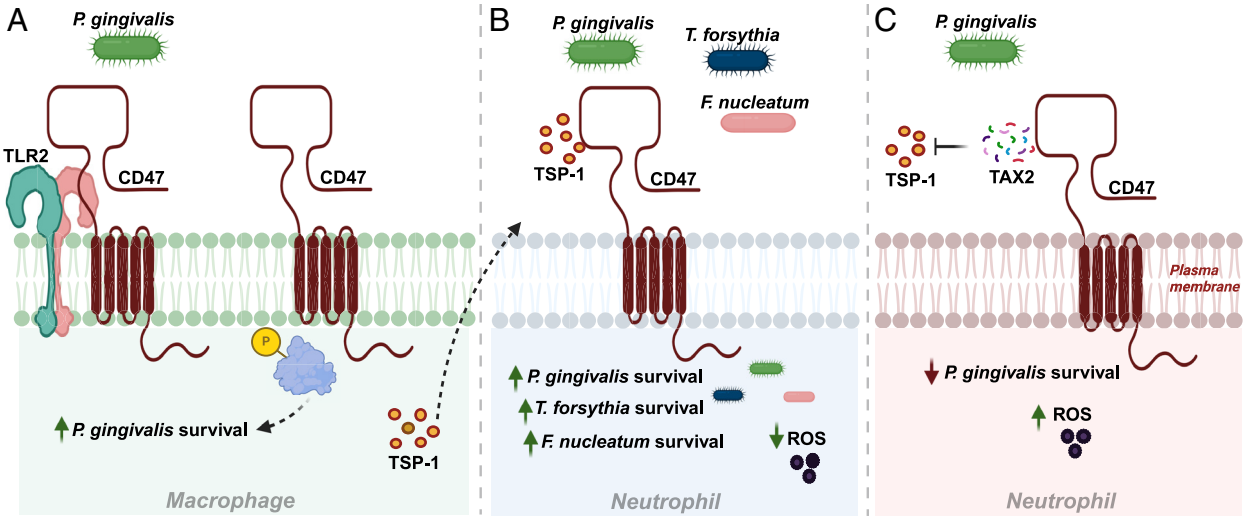

Fig. 8. Schematic illustration. TLR2–CD47 signaling induces AKT phosphorylation, enhanced intracellular survival, and TSP-1 secretion in macrophages in response to *P. gingivalis* (*A*). Secreted TSP-1 down-regulates neutrophil ROS and bactericidal activity (*B*) that is restored by blocking the interaction of TSP-1 with CD47 (*C*). Figure created with BioRender.com.

The oral microbiota is symbiotic when the gums are healthy. Together with an increase in species such as *P. gingivalis*, the microbiota shifts to a disease-associated state as the tissue becomes inflamed (52). Due to the link of oral microbial dysbiosis to systemic disease, interventions aimed at controlling the dysbiotic microbiome, and particular species that thrive in it such as *P. gingivalis* and *F. nucleatum*, can potentially improve health outcomes (33, 53, 54). *P. gingivalis* is considered a "keystone pathogen" since its presence directs the shift to a disease-provoking dysbiotic microbiota (55). Our finding that *P. gingivalis* infection induces TSP-1 secretion (Fig. 4 *E* and *F*) sheds light on the community-wide effects of *P. gingivalis* (55). In addition to live bacteria, LPS derived from *P. gingivalis* has also been shown to induce macrophage TSP-1 production (24, 44). Therefore, in periodontal lesions bacterial outer membrane vesicles or membrane fragments containing LPS are also likely drivers of TSP-1 production. TSP-1 expression has been shown to be downstream of AKT activation of NFκB in several cell types (56–58). We found that NFκB activation is necessary, but not sufficient, for TSP-1 induction in response to *P. gingivalis*. AKT signaling leads to activation of multiple transcription factors, in addition to NFκB (59, 60). Our findings suggest that CD47-TLR2 induction of AKT phosphorylation contributes additional signaling factors that are necessary for TSP-1 induction. Analysis of the TSP-1 promoter region [using PROMO (61) and EPD (62)] reveals candidate transcription factors that could explain this phenomenon such as CEB/Pβ that has been shown to be activated by PI3K/AKT signaling and induced by *P. gingivalis* (63, 64).

Secreted TSP-1 activates CD47 on naïve neutrophils leading to reduced killing of *P. gingivalis* and of other periodontitis-associated bacteria such as *F. nucleatum* and *T. forsythia* (Fig. 6 *C* and *D*). We found that TSP-1 reduces neutrophil ROS production leading to enhanced bacterial survival (Fig. 5 *C* and *F*). In *Klebsiella pneumoniae* pulmonary infection TSP-1 was shown to reduce neutrophil elastase and cathepsin G production diminishing intracellular microbial killing (65). Thus, TSP-1 may broadly impair neutrophil function in inflammatory lesions. Importantly, neutrophils encounter periodontal bacteria in the gingival crevice, and TSP-1 is elevated in the exudate (the gingival crevicular fluid) that reflects the environment within which the cells interact (29). We and others previously found that macrophages promote *P. gingivalis* survival by down-regulating neutrophil killing (39, 66). Specifically, ablation of $CX3CR1^{hi}$ monocyte/macrophages, a population known to produce TSP-1 (67), enhances neutrophil antibacterial activity and resistance to *P. gingivalis*–induced experimental periodontitis (39). Thus, TSP-1 is a candidate secreted factor that can explain how macrophages regulate hyperinflammatory neutrophils leading to ineffective clearance of periodontal pathogens, and how particular bacterial species can shape the microbiota by broadly affecting the host response to other species. Blocking TSP-1 activity via small molecule inhibitors such as the TAX2 peptide, represents a potential therapeutic strategy to improve neutrophil function and thereby counteract microbial dysbiosis. Interfering with bacterial immune evasion pathways instead of using antibiotics to control infection, is particularly attractive in periodontal disease since bacteria such as *P. gingivalis* persist chronically and are known to disseminate to distant sites where they promote systemic pathology (32, 33, 35).

Materials and Methods

Bacterial Culture. *P. gingivalis* (strain 381, American Type Culture Collection; ATCC) was used for all experiments except those involving the fimbriae mutants that were compared to their parent strain ATCC 33277. *P. gingivalis* 381 and *F. nucleatum* strain FC 23726 were cultured in Wilkins Chalgren Anaerobe Broth (Oxoid Ltd). *T. forsythia* strain FDC 338 was cultured with peptone and Yeast extract in BHI medium (Oxoid Ltd.), supplemented with 5% fetal calf serum (Biological Industries), hemin (5 μg/mL), vitamin k (0.5 μg/mL), and N-Acetylmuramic acid (10 μg/mL). *P. gingivalis* fimbriae mutants ΔFimA, ΔFimC, and ΔFimE were a kind gift from Prof. Jan Potempa (Jagiellonian University, Poland) and were constructed on the strain ATCC 33277 background. Mutants and WT strain 33277 were cultured in BHI blood agar or BHI broth supplemented with yeast extract (0.25%), hemin (5 μg/mL), vitamin k (1 μg/mL), and erythromycin (5 μg/mL) was added to the cultures of mutant strains. All bacteria were cultured under anaerobic conditions at 37 °C. For *P. gingivalis*, OD value of 0.1 at 650 nm was determined to correspond to 10^{10} CFU/mL, for *F. nucleatum,* OD value of 1 at 600 nm was determined to correspond to 10^9 CFU/ml, and for *T. forsythia,* OD value of 0.26 at 550 nm was determined to correspond to 10^9 CFU/mL. *P. gingivalis* (strain 33277) WT and FIM A mutant OD values of 1 at 600 nm was determined to correspond to 10^9 CFU/mL.

Mice. BALB/c OlaHsd and $CD47^{-/-}$ mice on a BALB/c OlaHsd background were used for this study. The $CD47^{-/-}$ mice were a kind gift from Prof. S. Rotshenker (Hebrew University, Israel). Mice were housed at the specific pathogen-free unit of the Hebrew University, Hadassah Medical School (Ein-Kerem, Jerusalem). All experiments were approved by the Institutional Animal Ethics Committee of the Hebrew University of Jerusalem (Permit No.: MD-11-13120-3) in compliance with the National Research Council guide for the care and use of laboratory animals (NIH Publication No. 85-23, revised 1996).

Subcutaneous Infection. As previously described (38, 39), two titanium coil chambers were subcutaneously inserted into the dorsum of 6- to 8-wk-old female mice. Seven days following implantation, chamber exudates were aspirated (baseline) and then 100 μL of 10^{10} *P. gingivalis* were inoculated into each chamber. At 2 h and 24 h postinfection, chamber exudates were aspirated, with each chamber of each mouse sampled at a different time point. *P. gingivalis* survival was determined by serial dilution plating on blood agar plates for CFU enumeration.

Cell Culture. Human macrophage THP1 cells (ATCC) were maintained in RPMI (Sigma Aldrich) supplemented with 10% fetal calf serum, 2 mM L-glutamine, penicillin (100 units/mL), streptomycin (100 μg/mL), 1% 1 M HEPES, and sodium pyruvate (Biological Industries). Cells were differentiated with 5 ng/mL phorbol 12-myristate 13-acetate (PMA, Sigma-Aldrich) for 72 h, to obtain mature macrophages. Raw 264.7 cells were maintained in Dulbecco's modified Eagle's medium (DMEM) (Sigma-Aldrich) supplemented with 10% fetal calf serum, 2 mM L-glutamine, penicillin (100 units/mL), and streptomycin (100 μg/mL) (Biological Industries). The cell lines were cultured at 37 °C and 5% CO_2 atmosphere. For inhibition of PI3K cells were treated with LY294002 or the control inhibitor LY303511 (MedChemExpress), and to inhibit NFκB cells were treated with BAY11-7082 (Sigma).

Isolation of Peripheral Blood Cell Subsets. Peripheral blood was drawn from healthy volunteers after informed consent was obtained (study approved by Hadassah Medical Organization Institutional Review Board). Neutrophils were isolated by density sedimentation using Ficoll-Paque (Amersham Biosciences) as per the manufacturer's instructions followed by RBC lysis. Neutrophil purity was confirmed to be ≥97% by CD66b staining. The purified PMNs were resuspended in RPMI and plated in 10 cm cell culture plates. Peripheral blood–derived monocytes were isolated by negative selection using the RosetteSep™ human monocyte enrichment cocktail (Stem cell technologies) before Ficoll-Paque density sedimentation. After centrifugation, the monocyte layer was obtained and washed with phosphate buffer saline (PBS) containing 1 mM ethylenediaminetetraacetic acid (EDTA) (pH 7.5). Cells were then differentiated to macrophages for 6 d with 20 ng/mL granulocyte-macrophage colony-stimulating factor (GM-CSF, PeproTech).

Coimmunoprecipitation and Immunoblotting. THP1 macrophages or TLR2-Flag transduced THP1 macrophages were infected with *P. gingivalis* at multiplicity of infection (MOI) 10 for 30 min. Cells were lysed in radioimmunoprecipitation assay (RIPA) buffer containing 150 mM NaCl, 20 mM Tris (pH 7.5), 1 mM EDTA, 1 mM EGTA, 1% NP-40, 1% sodium deoxycholate, protease, and phosphatase inhibitors (Sigma-Aldrich). Protein concentration was determined by bicinchoninic acid

(BCA) protein assay kit (Thermo Fisher Scientific). 1 μg protein was incubated with antibody coupled to protein G Dyna beads (Thermo Fisher Scientific). For THP1 cells, TLR2 was IP using anti-TLR2 clone T2.5 (Hycult Biotech), and for TLR2-Flag transduced THP1 the TLR2-Flag was precipitated using Ready Tag anti-DDDDK (BioXcel). Following immunoprecipitation bead complex was washed and resuspended in 1X Laemmli SDS sample buffer (Gene Bio Applications), boiled, and subjected to electrophoresis in precast 4 to 20% PAA gels (Gene Bio-Application, Ltd.). Membranes were blocked with freshly prepared 5% skim milk for 1 h and CD47 was detected with anti-CD47 antibody, 1:1,000 (GTX53912, GeneTex) incubated overnight at 4 °C followed by goat anti-rabbit IgG-HRP (Abcam).

Immunofluorescence. A total of 2×10^5 THP-1 cells were differentiated to macrophages on cover slips for 3 d. Cells were infected with *P. gingivalis* for 30 min, fixed with paraformaldehyde (PFA), and blocked with 5% bovine serum albumin (BSA). For coimmunofluorescence, cells were costained with primary antibodies to TLR2 (clone T2.5, 1:500) and CD47 (GTX53912, 1:500). To measure NFκB nuclear translocation, cells were stained with anti-rabbit NFκB p65 antibody (C-20, Santa Cruz) for P65 translocation experiment. Cells were washed and counterstained with Fluorescein (FITC) Goat Anti-Mouse IgG (H + L) (Jackson ImmunoResearch) and/or goat anti-rabbit IgG H&L (Alexa Fluor® 555) (Abcam). Images were obtained using a Nikon confocal microscope at 40× magnification. Colocalization analysis was performed using ImageJ. P65 cytoplasmic to nuclear translocation was calculated by the percentage of cells with nuclear p65 out of total number of cells per field (n = 5 fields scored per condition).

AKT Phosphorylation. THP-1 cells were differentiated to macrophages for 3 d and then incubated with serum-free medium for 3 h. Cells were then infected with *P. gingivalis* MOI 20 for 10 min followed by lysis in RIPA buffer. Protein concentration was determined by BCA and 5 μg protein was used for gel electrophoresis. Phosphorylated and total levels of Protein kinase B/AKT was detected using phospho-AKT(S473) antibody, 1:1,000 and AKT antibody (9272S), 1:1,000 (Cell Signaling Technology) primary antibodies and goat anti-rabbit IgG-HRP, 1:2,500 (Abcam) secondary antibody.

Phagocytosis. Bacteria (*P. gingivalis*, *T. forsythia,* and *F. nucleatum*) were labeled with fluorescein isothiocyanate (FITC) 0.1 mg/mL (Sigma-Aldrich) in carbonate buffer (pH 9.5) for 20 min at RT. Human neutrophils were infected with FITC-labeled bacteria for 30 min. Cells were thoroughly washed with PBS and extracellular florescence was quenched with 0.2% trypan blue (Sigma-Aldrich). Cells were then washed with PBS, fixed with 4% PFA, and analyzed on a Cytoflex cytometer (Beckman Coulter). Mean fluorescent intensity (MFI) was determined by FlowJo software (BD Biosciences).

Intracellular Survival Assay. Intracellular survival was determined using an antibiotic protection assay. A total of 10^6 cells/well were seeded in 6-well plates. Cells were then pretreated with blocking antibodies or recombinant protein for 1 h and 30 min, respectively, prior to challenge with *P. gingivalis* for 1 h. The extracellular bacteria were killed by incubating cells with 6 mg/mL Metronidazole (Sigma-Aldrich) and 0.3 mg/mL Gentamycin (Biological Industries) for 1 h. The medium was then replaced with complete medium and cells were incubated for 1 h prior to lysis in ice-cold sterile dd H_2O for 20 min, and lysates were plated on blood agar (Novamed) in anaerobic conditions at 37 °C for 7 to 10 d and CFU were enumerated.

qRT-PCR. Total RNA was extracted using TRIzol (Invitrogen, Thermo Fisher Scientific), according to the manufacturer's instructions, and quantified by spectrophotometry (Nanodrop One, Thermo Fisher Scientific). 0.5 μg RNA per sample was reverse-transcribed into cDNA using the qPCR BIO cDNA synthesis kit (PCRBIOSYSTEMS). qRT-PCR analysis was performed on a Bio-Rad CFX Connect system. The mRNA expression values were normalized to the house keeping GAPDH expression. qRT-PCR primers are listed in *SI Appendix*, Table S1.

ELISA. TNF-α levels were determined by the ELISA using mouse and human ELISA MAX TM sets (BioLegend), according to the manufacturer's instructions. TSP-1 levels were determined using the human Quantikine ELISA kit DTSP-10 (R&D systems) according to the manufacturer's instructions. For CD47 neutralization, anti-mouse CD47 miap 301 (20 μg/mL, Thermo Fisher Scientific) and anti-human CD47 clone B6H12 (10 μg/mL, BioXcel), were used. TLR2 was blocked using clone T2.5 at 20 μg/mL. Isotype control antibodies (rat IgG2a, and mouse IgG1, BioLegend) were used at equivalent concentrations. Blocking was performed for 1 h prior to *P. gingivalis* infection.

ROS Levels. Peripheral blood neutrophils were incubated for 30 min with human recombinant TSP-1 (R&D systems) and TAX2 peptide (100 μM, GeneCust) or a linear control peptide (100 μM) (68) for 1 h prior to bacterial infection for 1 h at 37 °C using rotation (69). Cells were washed with PBS and incubated with Dihydrorhodamine 123 (DHR-123; Sigma-Aldrich) for 15 min. DHR-123 conversion into the fluorophore rhodamine-123 (R-123) was detected using a TECAN Spark plate reader.

Flow Cytometry. The following antibodies were used: FITC-anti-CD47 clone miap410 (eBioscience), APC-anti-CD172a SIRP-a (eBioscience), and APC-anti-CD66B (Abcam). Cells were preincubated with FcR blocking reagent (Miltenyi Biotec) on ice and after labeling were fixed with 4% PFA. Cells were evaluated using a Cytoflex flow cytometer (Beckman Coulter), and data were analyzed by FlowJo software (BD Biosciences).

Statistical Analysis. Data were analyzed by two-tailed Student's *t* test or one-way ANOVA for multiple comparisons as indicated in the figure legends. Bars show mean and SD, and data were analyzed using Prism v.8, GraphPad Software Inc.

Data, Materials, and Software Availability. All study data are included in the article and/or *SI Appendix*.

ACKNOWLEDGMENTS. This study was supported by grants from the Israel Science Foundation (Grants 1391/17 and 2230/20 to G.N.). We acknowledge the assistance of Dr. Anat Blumenfeld in obtaining human samples and in critical review of the manuscript. We gratefully acknowledge the gift of the *Porphyromonas gingivalis* fimbriae mutants from Prof. Jan Potempa (Jagiellonian University, Krakow, Poland).

Author affiliations: [a]Institute of Biomedical and Oral Research, Hebrew University-Hadassah Faculty of Dental Medicine, Jerusalem 91120, Israel; and [b]Central Research Institute, Wakunaga Pharmaceutical Co. Ltd., Hiroshima 739-1195, Japan

1. G. Hajishengallis, Periodontitis: From microbial immune subversion to systemic inflammation. *Nat. Rev. Immunol.* **15**, 30–44 (2015).
2. C. Cugini, V. Klepac-Ceraj, E. Rackaityte, J. E. Riggs, M. E. Davey, *Porphyromonas gingivalis*: Keeping the pathos out of the biont. *J. Oral Microbiol.* **5**, 19804 (2013).
3. H. Makkawi *et al.*, *Porphyromonas gingivalis* stimulates TLR2-PI3K signaling to escape immune clearance and induce bone resorption independently of MyD88. *Front. Cell. Infect. Microbiol.* **7**, 359 (2017).
4. E. Harokopakis, M. H. Albzreh, M. H. Martin, G. Hajishengallis, TLR2 transmodulates monocyte adhesion and transmigration via Rac1- and PI3K-mediated inside-out signaling in response to *Porphyromonas gingivalis* fimbriae. *J. Immunol.* **176**, 7645–7656 (2006).
5. K. Pandi *et al.*, *Porphyromonas gingivalis* induction of TLR2 association with Vinculin enables PI3K activation and immune evasion. *PLoS Pathog.* **19**, e1011284 (2023).
6. E. Burns, G. Bachrach, L. Shapira, G. Nussbaum, Cutting edge: TLR2 is required for the innate response to *Porphyromonas gingivalis*: Activation leads to bacterial persistence and TLR2 deficiency attenuates induced alveolar bone resorption. *J. Immunol.* **177**, 8296–8300 (2006).
7. E. Burns, T. Eliyahu, S. Uematsu, S. Akira, G. Nussbaum, TLR2-dependent inflammatory response to *Porphyromonas gingivalis* is MyD88 independent, whereas MyD88 is required to clear infection. *J. Immunol.* **184**, 1455–1462 (2010).
8. M. Wang *et al.*, Microbial hijacking of complement-toll-like receptor crosstalk. *Sci. Signal.* **3**, ra11 (2010).
9. T. Maekawa *et al.*, *Porphyromonas gingivalis* manipulates complement and TLR signaling to uncouple bacterial clearance from inflammation and promote dysbiosis. *Cell Host Microbe* **15**, 768–778 (2014).
10. G. Hajishengallis, M. L. McIntosh, S. I. Nishiyama, F. Yoshimura, Mechanism and implications of CXCR4-mediated integrin activation by *Porphyromonas gingivalis*. *Mol. Oral. Microbiol.* **28**, 239–249 (2013).
11. G. Hajishengallis, M. Wang, S. Liang, M. Triantafilou, K. Triantafilou, Pathogen induction of CXCR4/TLR2 cross-talk impairs host defense function. *Proc. Natl. Acad. Sci. U.S.A.* **105**, 13532–13537 (2008).
12. E. Harokopakis, G. Hajishengallis, Integrin activation by bacterial fimbriae through a pathway involving CD14, Toll-like receptor 2, and phosphatidylinositol-3-kinase. *Eur. J. Immunol.* **35**, 1201–1210 (2005).
13. J. van Bergenhenegouwen *et al.*, TLR2 & Co: A critical analysis of the complex interactions between TLR2 and coreceptors. *J. Leukoc. Biol.* **94**, 885–902 (2013).
14. L. Barrera *et al.*, CD47 overexpression is associated with decreased neutrophil apoptosis/phagocytosis and poor prognosis in non-small-cell lung cancer patients. *Br. J. Cancer* **117**, 385–397 (2017).

15. M. C. Tal *et al.*, Upregulation of CD47 is a host checkpoint response to pathogen recognition. *mBio* **11**, e01293-20 (2020).
16. A. C. Chin *et al.*, CD47 and TLR-2 cross-talk regulates neutrophil transmigration. *J. Immunol.* **183**, 5957–5963 (2009).
17. A. Almubarak, K. K. K. Tanagala, P. N. Papapanou, E. Lalla, F. Momen-Heravi, Disruption of monocyte and macrophage homeostasis in periodontitis. *Front. Immunol.* **11**, 330 (2020).
18. M. Orazizadeh *et al.*, CD47 associates with alpha 5 integrin and regulates responses of human articular chondrocytes to mechanical stimulation in an in vitro model. *Arthritis Res. Ther.* **10**, R4 (2008).
19. T. Gianni, G. Campadelli-Fiume, The epithelial αvβ3-integrin boosts the MYD88-dependent TLR2 signaling in response to viral and bacterial components. *PLoS Pathog.* **10**, e1004477 (2014).
20. N. P. Podolnikova, S. Key, X. Wang, T. P. Ugarova, The CIS association of CD47 with integrin Mac-1 regulates macrophage responses by stabilizing the extended integrin conformation. *J. Biol. Chem.* **299**, 103024 (2023).
21. S. Takahashi, Molecular functions of SIRPα and its role in cancer. *Biomed. Rep.* **9**, 3–7 (2018).
22. A. Kale, N. M. Rogers, K. Ghimire, Thrombospondin-1 CD47 signalling: From mechanisms to medicine. *Int. J. Mol. Sci.* **22**, 4062 (2021).
23. K. Zen *et al.*, Inflammation-induced proteolytic processing of the SIRPα cytoplasmic ITIM in neutrophils propagates a proinflammatory state. *Nat. Commun.* **4**, 2436 (2013).
24. T. Xing *et al.*, Thrombospondin-1 production regulates the inflammatory cytokine secretion in THP-1 cells through NF-κB signaling pathway. *Inflammation* **40**, 1606–1621 (2017).
25. M. A. Morrissey, N. Kern, R. D. Vale, CD47 ligation repositions the inhibitory receptor SIRPA to suppress integrin activation and phagocytosis. *Immunity* **53**, 290–302.e296 (2020).
26. L. E. Métayer, A. Vilalta, G. A. A. Burke, G. C. Brown, Anti-CD47 antibodies induce phagocytosis of live, malignant B cells by macrophages. *Oncotarget* **8**, 60892–60903 (2017).
27. E. V. Stein, T. W. Miller, K. Ivins-O'Keefe, S. Kaur, D. D. Roberts, Secreted thrombospondin-1 regulates macrophage interleukin-1β production and activation through CD47. *Sci. Rep.* **6**, 19684 (2016).
28. J. E. Murphy-Ullrich, R. V. Iozzo, Thrombospondins in physiology and disease: New tricks for old dogs. *Matrix Biol.* **31**, 152–154 (2012).
29. X. Liu *et al.*, Targeting TSP-1 decreased periodontitis by attenuating extracellular matrix degradation and alveolar bone destruction. *Int. Immunopharmacol.* **96**, 107618 (2021).
30. M. A. Tayman *et al.*, A disintegrin-like and metalloproteinase with thrombospondin-1 (ADAMTS-1) levels in gingival crevicular fluid correlate with vascular endothelial growth factor-A, hypoxia-inducible factor-1α, and clinical parameters in patients with advanced periodontitis. *J. Periodontol.* **90**, 1182–1189 (2019).
31. M. A. Nazir, Prevalence of periodontal disease, its association with systemic diseases and prevention. *Int. J. Health Sci. (Qassim)* **11**, 72–80 (2017).
32. M. Muñoz-Medel *et al.*, A bridge between oral health and immune evasion in gastric cancer. *Front. Oncol.* **14**, 1403089 (2024).
33. E. Saba *et al.*, Oral bacteria accelerate pancreatic cancer development in mice. *Gut* **73**, 770–786 (2024).
34. X. Wang *et al.*, Promotes colorectal carcinoma by activating the hematopoietic. *Cancer Res.* **81**, 2745–2759 (2021).
35. S. S. Dominy *et al.*, In Alzheimer's disease brains: Evidence for disease causation and treatment with small-molecule inhibitors. *Sci. Adv.* **5**, eaau3333 (2019).
36. L. Li, R. Michel, J. Cohen, A. Decarlo, E. Kozarov, Intracellular survival and vascular cell-to-cell transmission of *Porphyromonas gingivalis*. *BMC Microbiol.* **8**, 26 (2008).
37. M. Wang *et al.*, Fimbrial proteins of *Porphyromonas gingivalis* mediate in vivo virulence and exploit TLR2 and complement receptor 3 to persist in macrophages. *J. Immunol.* **179**, 2349–2358 (2007).
38. A. Matsui *et al.*, Pathogenic bacterial species associated with endodontic infection evade innate immune control by disabling neutrophils. *Infect. Immun.* **82**, 4068–4079 (2014).
39. O. Steinmetz *et al.*, CX3CR1hi monocyte/macrophages support bacterial survival and experimental infection-driven bone resorption. *J. Infect. Dis.* **213**, 1505–1515 (2016).
40. K. Pandi *et al.*, *P. gingivalis*-induced TLR2 interactome analysis reveals association with PARP9. *J. Dent. Res.* **103**, 329–338 (2024).
41. N. Wara-aswapati *et al.*, Induction of toll-like receptor expression by *Porphyromonas gingivalis*. *J. Periodontol.* **84**, 1010–1018 (2013).
42. P. Leclair, C. J. Lim, CD47 (Cluster of differentiation 47): An anti-phagocytic receptor with a multitude of signaling functions. *Anim. Cells Syst. (Seoul)* **24**, 243–252 (2020).
43. A. Jeanne *et al.*, Identification of TAX2 peptide as a new unpredicted anti-cancer agent. *Oncotarget* **6**, 17981–18000 (2015).
44. M. Gokyu *et al.*, Thrombospondin-1 production is enhanced by *Porphyromonas gingivalis* lipopolysaccharide in THP-1 cells. *PLoS ONE* **9**, e115107 (2014).
45. C. Martin-Gallausiaux, A. Malabirade, J. Habier, P. Wilmes, Extracellular vesicles modulate gut epithelial cell innate immunity. *Front. Immunol.* **11**, 583644 (2020).
46. Y. P. Jia *et al.*, TLR2/TLR4 activation induces Tregs and suppresses intestinal inflammation caused by *Fusobacterium nucleatum* in vivo. *PLoS ONE* **12**, e0186179 (2017).
47. S. R. Myneni *et al.*, TLR2 signaling and Th2 responses drive *Tannerella forsythia*-induced periodontal bone loss. *J. Immunol.* **187**, 501–509 (2011).
48. L. Oliveira-Nascimento, P. Massari, L. M. Wetzler, The role of TLR2 in infection and immunity. *Front. Immunol.* **3**, 79 (2012).
49. E. J. Brown, W. A. Frazier, Integrin-associated protein (CD47) and its ligands. *Trends Cell Biol.* **11**, 130–135 (2001).
50. M. Kaneko *et al.*, Toll-like receptor-2 has a critical role in periodontal pathogen-induced myocardial fibrosis in the pressure-overloaded murine hearts. *Hypertens. Res.* **40**, 110–116 (2017).
51. C. H. Heldin, B. Lu, R. Evans, J. S. Gutkind, Signals and receptors. *Cold Spring Harb. Perspect. Biol.* **8**, a005900 (2016).
52. G. Hajishengallis, R. J. Lamont, Polymicrobial communities in periodontal disease: Their quasi-organismal nature and dialogue with the host. *Periodontology 2000* **86**, 210–230 (2021).
53. J. L. Baker, J. L. Mark Welch, K. M. Kauffman, J. S. McLean, X. He, The oral microbiome: Diversity, biogeography and human health. *Nat. Rev. Microbiol.* **22**, 89–104 (2024).
54. Z. Lan *et al.*, The role of oral microbiota in cancer. *Front. Microbiol.* **14**, 1253025 (2023).
55. G. Hajishengallis, R. P. Darveau, M. A. Curtis, The keystone-pathogen hypothesis. *Nat. Rev. Microbiol.* **10**, 717–725 (2012).
56. M. D. Tran, J. T. Neary, Purinergic signaling induces thrombospondin-1 expression in astrocytes. *Proc. Natl. Acad. Sci. U.S.A.* **103**, 9321–9326 (2006).
57. J. Trink *et al.*, Cell surface GRP78 regulates TGFβ1-mediated profibrotic responses. *Front. Pharmacol.* **14**, 1098321 (2023).
58. M. Abdalla *et al.*, The Akt inhibitor, triciribine, ameliorates chronic hypoxia-induced vascular pruning and TGFβ-induced pulmonary fibrosis. *Br. J. Pharmacol.* **172**, 4173–4188 (2015).
59. T. Mantamadiotis, Towards targeting PI3K-dependent regulation of gene expression in brain cancer. *Cancers (Basel)* **9**, 60 (2017).
60. A. T. Jalil *et al.*, Phosphatidylinositol 3-kinase signaling pathway and inflammatory bowel disease: Current status and future prospects. *Fundam. Clin. Pharmacol.* **37**, 910–917 (2023).
61. D. Farré *et al.*, Identification of patterns in biological sequences at the ALGGEN server: PROMO and MALGEN. *Nucleic Acids Res.* **31**, 3651–3653 (2003).
62. R. Dreos, G. Ambrosini, R. C. Périer, P. Bucher, The Eukaryotic Promoter Database: Expansion of EPDnew and new promoter analysis tools. *Nucleic Acids Res.* **43**, D92–D96 (2015).
63. Y. Bai, Y. Wei, L. Wu, J. Wei, X. Wang, C/EBP β mediates endoplasmic reticulum stress regulated inflammatory response and extracellular matrix degradation in LPS-stimulated human periodontal ligament cells. *Int. J. Mol. Sci.* **17**, 385 (2016).
64. H. Li *et al.*, PTPN14 promotes gastric cancer progression by PI3KA/AKT/mTOR pathway. *Cell Death Dis.* **14**, 188 (2023).
65. Y. Zhao *et al.*, Thrombospondin-1 restrains neutrophil granule serine protease function and regulates the innate immune response during *Klebsiella pneumoniae* infection. *Mucosal Immunol.* **8**, 896–905 (2015).
66. R. S. Lam *et al.*, Macrophage depletion abates *Porphyromonas gingivalis*-induced alveolar bone resorption in mice. *J. Immunol.* **193**, 2349–2362 (2014).
67. P. Lu *et al.*, Protective roles of the fractalkine/CX3CL1–CX3CR1 interactions in alkali-induced corneal neovascularization through enhanced antiangiogenic factor expression. *J. Immunol.* **180**, 4283–4291 (2008).
68. S. Dishon *et al.*, Development of a novel backbone cyclic peptide inhibitor of the innate immune TLR/IL1R signaling protein MyD88. *Sci. Rep.* **8**, 9476 (2018).
69. M. E. Mulcahy *et al.*, Manipulation of autophagy and apoptosis facilitates intracellular survival of *Staphylococcus aureus* in human neutrophils. *Front. Immunol.* **11**, 565545 (2020).